The β_{2a} Subunit Is a Molecular Groom for the Ca^{2+} Channel Inactivation Gate

S. Restituito,[1] T. Cens,[1] C. Barrere,[1] S. Geib,[2] S. Galas,[1] M. De Waard,[2] and P. Charnet[1]

[1]*Centre de Recherches de Biochimie Macromoléculaire, Centre National de la Recherche Scientifique, Unité Propre de Recherche 1086, Institut Fédératif de Recherche 24, 34293 Montpellier Cedex 05, France, and* [2]*Institut National de la Santé et de la Recherche Médicale U464, Institut Fédératif Jean Roche, Laboratoire de Neurobiologie des Canaux Ioniques, 13916 Marseille Cedex 20, France*

Ca^{2+} channel inactivation is a key element in controlling the level of Ca^{2+} entry through voltage-gated Ca^{2+} channels. Interaction between the pore-forming α_1 subunit and the auxiliary β subunit is known to be a strong modulator of voltage-dependent inactivation. Here, we demonstrate that an N-terminal membrane anchoring site (MAS) of the β_{2a} subunit strongly reduces α_{1A} ($Ca_V2.1$) Ca^{2+} channel inactivation. This effect can be mimicked by the addition of a transmembrane segment to the N terminus of the β_{2a} subunit. Inhibition of inactivation by β_{2a} also requires a link between MAS and another important molecular determinant, the β interaction domain (BID). Our data suggest that mobility of the Ca^{2+} channel I–II loop is necessary for channel inactivation. Interaction of this loop with other identified intracellular channel domains may constitute the basis of voltage-dependent inactivation. We thus propose a conceptually novel mechanism for slowing of inactivation by the β_{2a} subunit, in which the immobilization of the channel inactivation gate occurs by means of MAS and BID.

Key words: P/Q type Ca^{2+} channels; $Ca_V2.1$; β subunit; inactivation mechanism; palmitoylation; membrane anchoring; I–II loop

Ca^{2+} channels β subunits are intracellular proteins associated *in vivo* with high voltage-activated Ca^{2+} channel α_1 subunits, which finely tune many of their electrophysiological and kinetic properties (Berrow et al., 1997). Ten different genes encode voltage-gated Ca^{2+} channel α_1 subunits (Randall and Benam, 1999). All of them, except the T-type Ca^{2+} channels (Randall and Benam, 1999), can interact with one of four different β subunits (β_1–β_4) (Birnbaumer et al., 1998; Walker and De Waard, 1998). Within the same type of pharmacologically defined Ca^{2+} channels, these β subunits represent a major determinant of variability in channel properties. β_1, β_3, and β_4 subunits induce hyperpolarizing shifts in the activation and inactivation properties of these channels and accelerate their activation kinetics and voltage- and Ca^{2+}-dependent inactivation (Varadi et al., 1991; Neely et al., 1993; Sather et al., 1993; Stea et al., 1993; Jones et al., 1998). The β_{2a} subunit plays a different role because it slows down voltage- and Ca^{2+}-dependent inactivation (Sather et al., 1993; Stea et al., 1994; Jones et al., 1998) and is unable to confer prepulse facilitation to the L-type Ca^{2+} channel (Cens et al., 1996). Sequence homology analysis of these different β subunits reveals the existence of two well conserved domains in their primary sequence (C1, C2), surrounded by more variable regions in which alternative splicing occurs (V1–V3) (Fig. 1) (Perez Reyes and Schneider, 1994). The conserved site of interaction between the α_1 and the β subunits has been mapped to the beginning of the C2 domain of β (De Waard et al., 1994; Walker and De Waard, 1998). This site interacts with a consensus β subunit-binding sequence [α interaction domain (AID)] localized on the loop connecting domain I and II of the α_1 subunit (Pragnell et al., 1994; De Waard et al., 1995). The specificity of the effects of the β_{2a} subunit is mediated, as least in part, by two cysteines located at the N terminal end of some isoforms of the β_{2a} subunits (Fig. 1) (Chien et al., 1996; Qin et al., 1998). Similar to α_s GTP-binding proteins, these cysteines are post-translationally modified through the addition of thioester-bound palmitic acids and thus allow a membrane association of the β_{2a} subunit (Chien et al., 1998) and regulation of the inactivation of the α_{1E} subunit (Qin et al., 1998). However, the partial data available have not yet allowed the elucidation of the molecular mechanisms by which these palmitoylated cysteines slow inactivation.

In this work, we have expressed several mutated forms of the β_1 and β_2 subunits in *Xenopus* oocytes and tsA 201 cells and analyzed in parallel (1) their effects on the inactivation of P/Q type Ca^{2+} channels, and (2) their subcellular localization when expressed alone. Our results strongly suggest that the β_{2a} subunit acts as an anchor for the Ca^{2+} channel I–II loop proposed to be an inactivation particle, thus reducing inactivation. We show that several intracellular domains of the α_{1A} ($Ca_V2.1$) channel can interact with the I–II loop and are thus potential receptor sites for the inactivation particle.

MATERIALS AND METHODS

Preparation of mutated β subunits. The following calcium channel subunits were used: α_{1A} (Starr et al., 1991), β_{1b} (Pragnell et al., 1991), β_{2a} (Perez Reyes et al., 1992), and α_2-δ. All of these cDNAs were inserted into the pMT2 expression vector (Stea et al., 1994). Chimeras were produced by a classical two-step PCR approach (Cens et al., 1998). βTF1 and β chimera were finally digested using *Eco*RI and *Xba*I and subcloned into pBluescript (Stratagene, La Jolla, CA) before sequencing (DiDeoxy Terminator technology; Applied Biosystems, Foster City, CA). Constructs were subsequently subcloned into pMT2 for injection and expression.

Point mutants were obtained by PCR following commercial mutagenesis kit instructions (Quick Change site-directed mutagenesis kit; Stratagene) and using the following sense and antisense primers: β_2C3,4S AS, ATG TAC CAG CCC GGA GGA CTG CAT GAA GAG GTG G; β_2 C3S AS, ATG TAC CAG CCC GCA GGA CTG CAT GAA GAG GTG G; β_2 C4S AS, ATG TAC CAG CCC GGA GCA CTG CAT GAA GAG GTG G; β_2R9–11A AS, GGA CAC CCG TAC TGC CGC GGC ATG TAC CAG CCC G; β_2R10A AS, CCG TAC TGC CGC GCG ATG TAC; and β_2R13A AS, CCA TAG GAC ACC GCT ACT CGC CGG.

For the chimera CD8-β_{2a}C3,4S construction, the β_{2a} was amplified from

Received July 7, 2000; revised Sept. 29, 2000; accepted Oct. 13, 2000.

This work was supported by Centre National de la Recherche Scientifique, Institut National de la Santé et de la Recherche Médicale, the Association Française contre les Myopathies, the Association pour la Recherche contre le Cancer, the Fondation pour la Recherche Médicale, Ligue Nationale contre le Cancer, and the Groupe de Reflexion sur la Recherche Cardiovasulaire. We thank Drs. T. Snutch and E. Perez-Reyes for kindly providing calcium channel cDNAs, Dr. J. Streissnig for β-com antibody, Drs. J. Mery and A. Chavanieux for peptide synthesis, and Drs. N. Morin, I. Lefèvre, A. Gouin-Charnet, J.-C. Labbé, and N. Lautredau (Centre for Research on Innovation and Competition) for invaluable technical help during the course of these experiments.

Correspondence should be addressed to Dr. Pierre Charnet, Centre de Recherches de Biochimie Macromoléculaire, Centre National de la Recherche Scientifique, Unité Propre de Recherche 1086, Institut Fédératif de Recherche 24, 1919 Route de Mende, 34293 Montpellier Cedex 05, France. E-mail: charnet@crbm.cnrs-mop.fr.

 0270-6474/00/209046-07$15.00/0

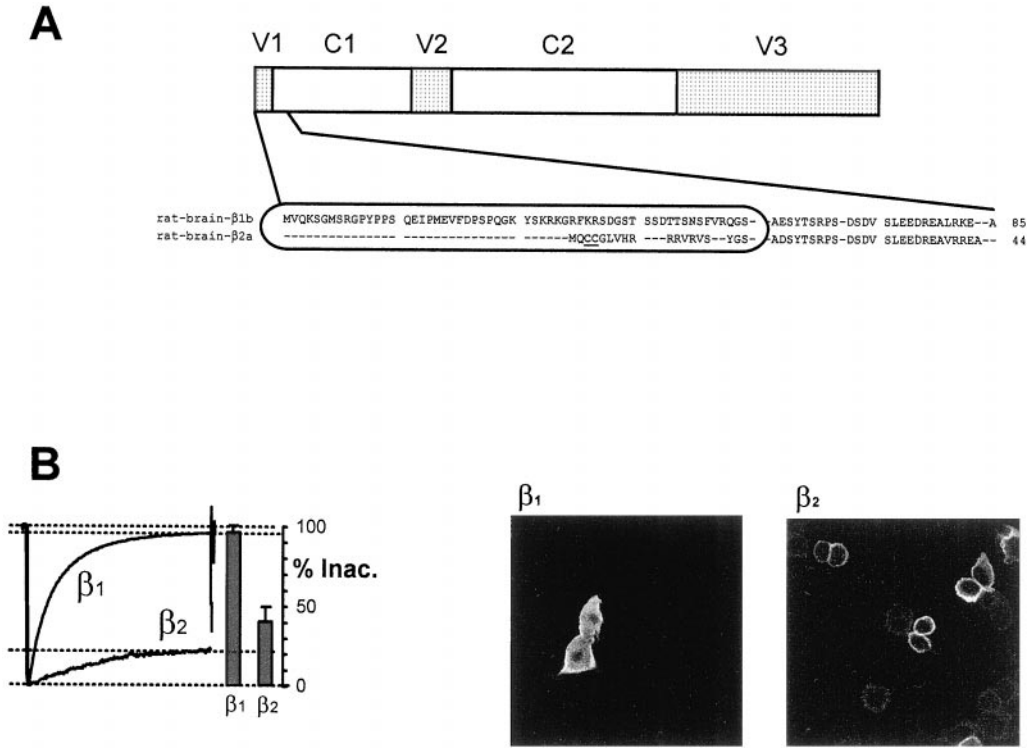

Figure 1. *A*, Schematic representation of the Ca^{2+} channel β subunit. *V1*, *V2*, and *V3* represent regions of variable sequences among the different β subunits. *C1* and *C2* are regions of high homology. Drawing has been scaled according to β_{2a} sequence, and the *box* represents the V1 sequence. Amino acid alignment of the N-terminal tail of the β_1 and β_2 subunits. Note the presence of the two Cys residues in the rat β_2 subunit. *B*, *Left*, Rapidly and slowly inactivating Ba^{2+} currents recorded from oocytes expressing the α_{1A} plus α_2-δ calcium channel subunits with, respectively, the β_1 or the β_2 subunits. Inactivation was quantified by the percent of inactivation measured at the end of a 2.5 sec test pulse to +10 mV. *Right*, Confocal immunofluorescent images of β subunit-transfected tsA 201 cells were obtained after fixation and immunohistochemical staining using a β-com primary antibody. Note the membrane localization of the β_{2a} subunit while the β_1 subunit is localized to the cytoplasm.

the pMT2 vector by PCR, using a forward primer containing the double cysteine mutation. The following primers were used: forward, 5′-CGCGGATCCCAGTCCTCCGGGCTGGTACATCGCCGGCGAGTACGG-3′, and reverse, 5′-ACGTGAATTCTTGGCGGATGTATACATCCCTGTTCCACTCGCCGAC-3′, containing *Bam*HI or *Eco*RI restriction sites, respectively.

The PCR product was purified and subcloned in frame into the *Bam*HI and *Eco*RI sites of the pcDNA3-CD8-βARK-Myc vector after removing the βARK insert. This vector was generously provided by Dr. J. Lang (Geneva University, Geneva, Switzerland).

In vitro *translation and binding of glutathione* S-*transferase fusion proteins.* ^{35}S-labeled α_{1A} I–II loop was synthesized by coupled *in vitro* transcription and translation (TNT; Promega, Madison, WI). Purified glutathione *S*-transferase (GST) fusion proteins (250 nM each) were immobilized to glutathione agarose beads (Sigma-Aldrich, Saint Quentin Fallavier, France) by 30 min incubation in TBS (25 mM Tris and 150 mM NaCl, pH 7.4) and 0.1% Triton X-100. Binding was initiated by addition of the ^{35}S-labeled α_{1A} I–II loop (2 μl), and this final mixture was incubated overnight at 4°C. Beads were washed four times with binding buffer, and associated ^{35}S-labeled α1A I–II loop was analyzed by SDS-PAGE and autoradiography.

Cell transfection and immunofluorescence. tsA 201 cells were maintained in DMEM (Life Technologies, Rockville, MD) containing 10% fetal bovine serum and 1% penicillin–streptomycin at 37°C in 5% CO_2. Transfections were performed using Superfect according to the protocols of Qiagen (Hilden, Germany), 1 d after plating the cells on poly-L-ornithine-treated 35 mm Petri dishes. Plasmid cDNA(s) (5 μg) was used for each transfection with an incubation time of 2 hr. Forty-eight hours later, cells were fixed and permeabilized using PBS supplemented with 4% paraformaldehyde and 0.05% Triton X-100 (20 and 10 min, respectively). After an incubation of 1 hr in 3% PBS plus BSA, cells were incubated an additional 1 hr with the primary polyclonal antibody β-com (Pichler et al., 1997), washed three times in PBS, and incubated 1 hr with the secondary anti-rabbit goat antibody conjugated to CY-3 (Sigma-Aldrich). After three other washes, cells were mounted and viewed on a conventional or a confocal immunofluorescent microscope. Confocal microscopy was performed at the CRIC (Center Régional d'Imagerie Cellulaire) facilities.

Xenopus *oocyte preparation and injection. Xenopus* oocyte preparation and injection (5–10 nl of α_1, α_1 plus β, or α_1 plus $\alpha_2\delta$ plus β cDNAs at ~ 0.3 ng/nl) were performed as described previously (Cens et al., 1996). Oocytes were then incubated for 2–7 d at 19°C under gentle agitation before recording.

Electrophysiological recordings. Whole-cell Ba^{2+} currents were recorded under two-electrode voltage clamp using a GeneClamp 500 amplifier (Axon Instruments, Burlingame, CA). Current and voltage electrodes (<1 MΩ) were filled with CsCl 2.8 M and BAPTA 10 mM, pH 7.2 with CsOH. Ba^{2+} current recordings were performed after injection of BAPTA [~50 nl of (in mM): 100 BAPTA-free acid (Sigma-Aldrich), 10 CsOH, and 10 HEPES, pH 7.2 with CsOH using one or two 40–70 msec injection at 1 bar] in the following bath solution (in mM): 10 BaOH, 20 TEAOH, 50 NMDG, 2 CsOH, and 10 HEPES, pH 7.2 with methanesulfonic acid. Ba^{2+} current amplitudes were usually in the range of 1–5 μA. Currents were filtered and digitized using a DMA-Tecmar Labmaster (Tecmar Inc., Longmont, CO) and subsequently stored on a IPC 486 personal computer using version 6.02 of the pClamp software (Axon Instruments). Ba^{2+} currents were recorded during a typical 2.5 sec duration test pulse from −80 to +10 mV. Current amplitudes were measured at the peak of the current (I_1) and at the end of the pulse (I_2). The percentage of inactivation was calculated as the ratio $(I_1 - I_2)/I_1$. Pseudo steady-state inactivation (2.5 sec of conditioning depolarization followed by a 400 msec test pulse to +10 mV) was fitted using the following equation:

$$I/I_{max} = R + (1 - R)/(1 + \exp((V - V_{0.5})/k))$$

where I is the current amplitude measured during the test pulse at +10 mV for conditioning depolarizations varying from −80 to +50 mV, I_{max} is the current amplitude measured during the test pulse for a conditioning depolarization of −80 mV, R is the proportion of non-inactivating current, V is the conditioning depolarization, $V_{0.5}$ is the half-inactivation potential, and k is a slope factor. Similar inactivation curves were also performed using 7.5 sec conditioning depolarizations without significant differences in the calculated $V_{0.5}$. All values are presented as mean ± SD of n determinations. A Student's t test was used at $p = 0.05$ to determine the significance of the difference between the two means.

RESULTS

Coexpression of the α_{1A} and α_2-δ subunits with the neuronal β_{1b} in *Xenopus* oocytes resulted in a Ba^{2+} current that inactivated by >90% after 2.5 sec (93 ± 2%) (Fig. 1*B*). A similar experiment performed with the β_{2a} subunit produced Ba^{2+} currents with very slow inactivation kinetics leading to only 40 ± 9% inactivation at the end of the pulse (Fig. 1). Because expression of the α_{1A} subunit alone gave currents with fast inactivation (Mangoni et al., 1997), we interpreted this slowing in the presence of the β_{2a} subunit as a blocking of the normal inactivation mechanism. Moreover, the β_{1b} subunit that provided rapidly inactivating currents (when expressed with the α_{1A} subunit) was localized throughout the cytoplasm (when expressed alone), whereas the β_{2a} subunit that produced slow currents was localized close to the membrane (Fig. 1*B*). We and others have shown that the V1 domain of the β_{2a} subunit (in which palmitoylation occurs) (Fig. 1) is the main determinant of the β_{2a} subunit-induced regulation of voltage- and Ca^{2+}-dependent inactivation, as well as of the inhibition of facilitation of the α_{1C} Ca^{2+} channel (Olcese et al., 1994; Cens et al., 1998, 1999a,b; Qin et al., 1998). However, although palmitoylation of the

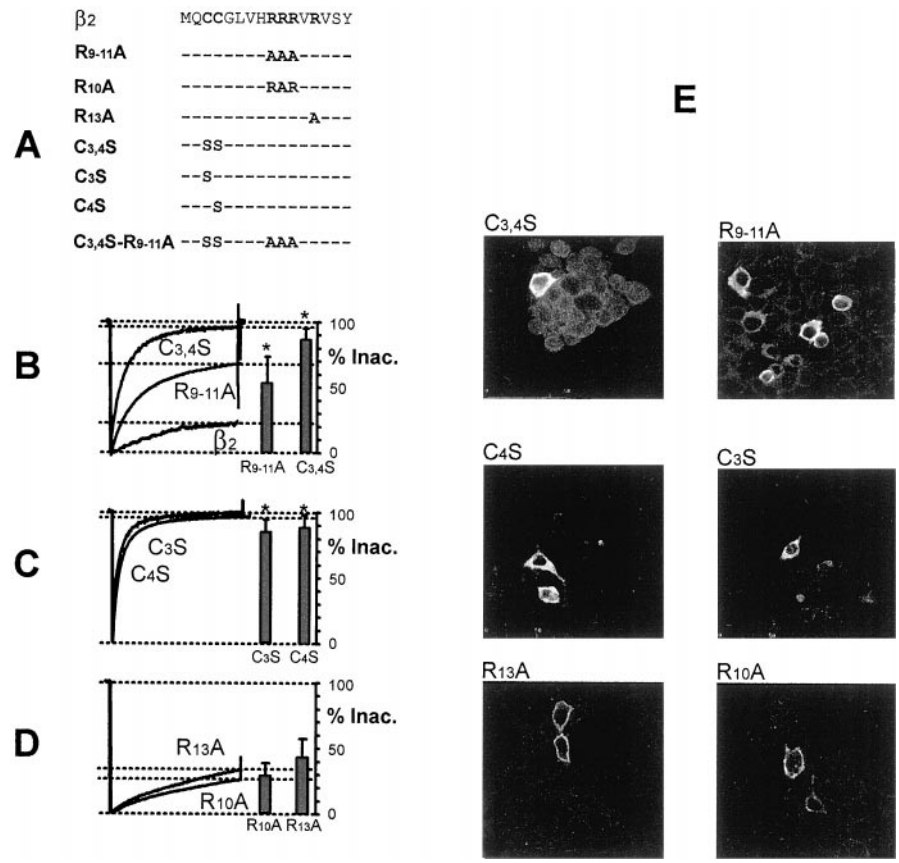

Figure 2. Cys3 and Cys4 of β_2 are major determinants for membrane localization and slow inactivation. *A*, Localization and nature of the different mutations made in the V1β_2 domain. β_2 refers to the wild-type sequence of the rat β_{2a} subunit. *B*, Mutation of Cys(3,4) of the β_{2a} subunit to Ser (labeled *C3,4S* in *B*) induced a marked increase in inactivation ($n = 21$) and a localization of the β_{2a} subunit to the cytoplasm (see *E*). Mutation of Arg(9,10,11) to Ala (labeled *R9–11A* in Fig. 3*B*; $n = 13$) has a similar, albeit reduced in amplitude, effect: acceleration of the inactivation kinetics and cytoplasmic localization of the mutated β_{2a} subunit (see *E*). *Traces* labeled β_2 show current kinetics recorded with the wild-type β_{2a} subunit (similar to *trace* labeled β_2 in Fig. 1*B*) for comparison. * indicates statistically different from β_2. *C*, Mutation of only one Cys to Ser (either Cys3, $n = 14$; or Cys4, $n = 7$; labeled *C3S* and *C4S*, respectively) is sufficient to produce an acceleration of current kinetics and a delocalization of the mutated β_{2a} subunit to the cytoplasm (see *E*). * indicates statistically different from β_2. *D*, However, mutation of only one Arg (either Arg(10)Ala, $n = 19$; or Arg(13)Ala, $n = 9$; labeled *R10A* and *R13A*, respectively) has no effect on current kinetics (*left*) and membrane localization (*right*) of the β subunit (*E*). *E*, Confocal immunofluorescent images of tsA 201 cells transfected with the different mutated β_{2a} subunits.

β_{2a} subunit has been shown recently to be involved in both membrane association of the subunit and slowing of the inactivation kinetics, the causal relation between these phenomena has not been studied.

Simultaneous mutations of Cys3 and Cys4 to Ser residues (designated β_2C3,4S) (Fig. 2*A*) has been shown to prevent β_{2a} subunit palmitoylation in *Xenopus* oocytes and to accelerate α_{1E} Ca^{2+} channel inactivation (Chien et al., 1998; Qin et al., 1998). When expressed in oocytes with the α_{1A} subunit, we also observed this increase in inactivation (87 ± 13% compared with 40% for β_{2a}) (Fig. 2*B*). Figure 2*E* shows that expression of this mutated subunit was diffuse in the cytoplasm. Interestingly, expression of single Cys mutations of the β_{2a} subunit, either Cys3 (β_2C3S) or Cys4 (β_2C4S), produced a similar effect on both the Ca^{2+} channel inactivation (85 ± 7 and 87 ± 17%, respectively) and the intracellular localization of the β_{2a} subunit (Fig. 2*E*), suggesting that both Cys residues need to be present for a correct palmitoylation of the β_{2a} subunit. Mutation of positively charged residues Arg10 and Arg13 of the β_{2a} subunit (β_2R10A and β_2R13A, respectively) (Fig. 2*D*) had no effect on channel inactivation (30 ± 11 and 47 ± 20%) or on β subunit localization, which remained, for both mutations, membrane localized (Fig. 2*E*). However, when the three Arg residues at positions 9, 10, and 11 of the β_{2a} subunit were replaced by Ala residues (mutant β_2R9–11A) (Fig. 2), the membrane association of the β_{2a} subunit was lost (Fig. 2*B*,*E*). Recordings of Ca^{2+} currents in the presence of this mutant showed that the inactivation kinetics of the α_{1A} Ca^{2+} channel were significantly faster than with the β_{2a} subunit (51 ± 22%). Therefore, additional sites other than the two Cys are important for the proper membrane association and slowing of inactivation induced by the β_{2a} subunit. If we postulate that membrane association of the β_{2a} subunit, when expressed alone, was attributable to palmitoylation of Cys3 and Cys4, mutation R9–11A could affect either the formation and the stability of the thioester bond or the association with the plasma membrane through modification of electrostatic interactions as already shown in the case of Src (Murray et al., 1998). Indeed, the double mutant (β_2C3,4S-R9–11A), which lacks both the two Cys residues and the three Arg residues (Fig. 2) and therefore cannot be palmitoylated, displayed current inactivation kinetics and subcellular localization identical to the βC3,4S mutant (94 ± 2% and cytoplasm localization; data not shown).

Altogether, these data suggest that multiple sites can affect the palmitoylation level and the cellular localization of the β_{2a} subunit. In all cases, however, the membrane localization of the β subunit was always associated with a marked slowing of the inactivation kinetics, suggesting that this feature represents a key element for slow inactivation. We tested this idea by forcing the membrane localization of the subunit by addition of a transmembrane segment at the N terminal tail of the double Cys-mutated β subunit. The resulting chimera (CD8-β_2C3,4S) (Fig. 3*A*) possessed the transmembrane sequence of the CD8 protein in the N-terminal position. We expressed this chimeric protein in *Xenopus* oocytes along with the α_{1A} and $\alpha_2\delta$ subunits for current recordings or alone in tsA 201 cells to study its cellular localization. As shown in Figure 3*B*, addition of the CD8 sequence produced a very marked slowing of the inactivation kinetics (33 ± 14% compared with 87 ± 12% to the β_2C3,4S mutant). In other terms, the forced membrane localization of the protein restored a key regulation that is normally seen with the wild-type β_{2a} subunit but not with the double Cys mutated form of the protein. This characteristic slowing in inactivation induced by the CD8-β_2C3,4S chimera was quite expectedly correlated with a membrane association of the protein as detected by immunofluorescence staining using either an anti-β (Fig. 3*C*) or an anti-CD8 antibody (data not shown). Similar results were found with the CH4 subunit, a chimeric β_1 subunit with the first V1 domain replaced by the homologous domain of the β_2 subunit. The slow current inactivation (Olcese et al., 1994) and membrane localization induced by CH4 (Fig. 3*B*) is only attributable to the V1 domain of β_2, because a β_1 subunit from which this domain has been deleted (β_1TF1) kept its cytoplasmic localization and still induced fast inactivation (88 ± 4% of inactivation; data not shown). Thus, mutation of Cys3 and Cys4 in CH4 accelerates

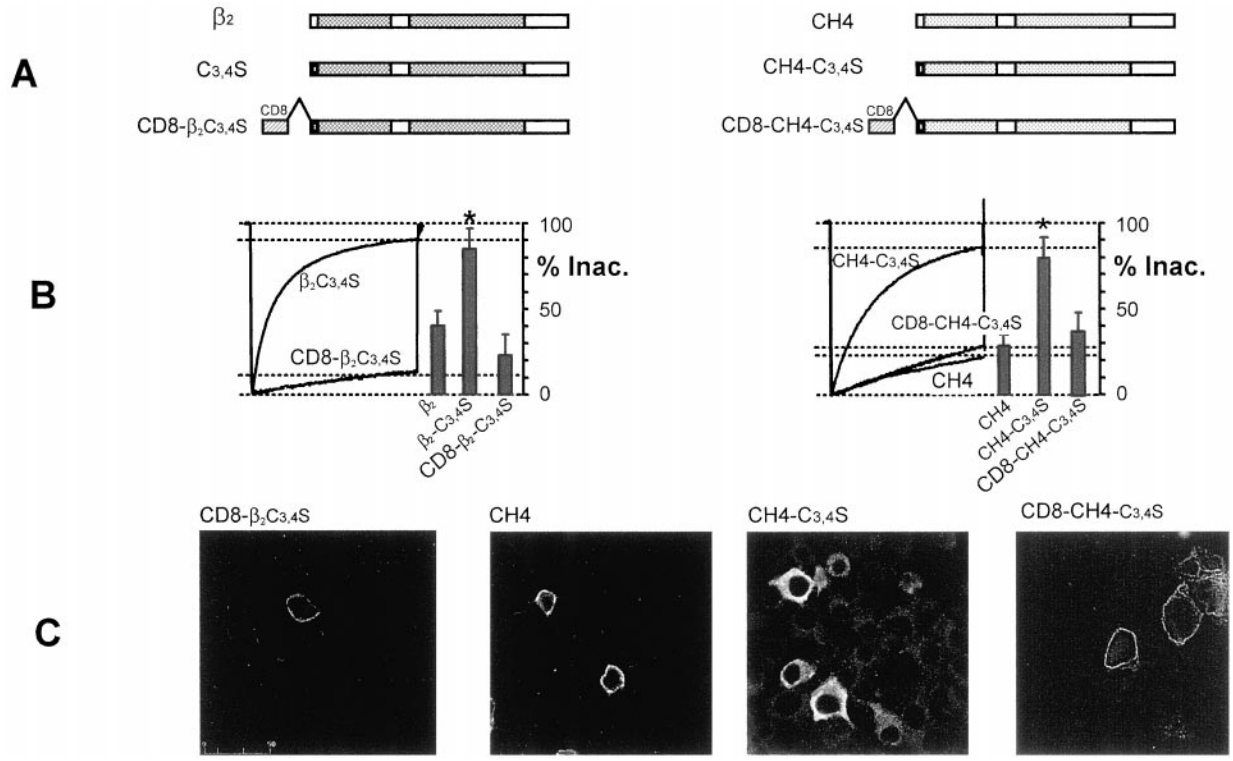

Figure 3. Addition of a membrane-spanning sequence at the N-terminal end of β_2*C3,4S* slows inactivation. *A*, Schematic representation of the CD8 constructions. The ectomembrane and transmembrane domains of the CD8 receptor were fused to the N-terminal end of the β_2C3,4S subunit, giving the chimeric CD8-β_2C3,4S subunit. Similarly CD8-CH4-C3,4S was constructed using the mutated Cys3,4S CH4 chimera (in which the V1 domain of β_1 was replaced by V1β_2). *B*, Ba^{2+} currents recorded from oocytes expressing the α_{1A} and α_2-δ subunits with the β_2C3,4S, the CD8-β_2C3,4S, the CH4, the CH4-C3,4S, or the CD8-CH4-C3,4S subunits. Mutation Cys(3,4)Ser in β_2 induced a rapidly inactivating currents (labeled *C3,4S*; $n = 21$), correlated with a cytoplasmic localization, as seen in Figure 3. Addition of the CD8 receptor transmembrane segment (CD8-β_2C3,4S; $n = 8$) restored the slow inactivation typically seen with the wild-type β_{2a} subunit. * indicates statistically different from β_2C3,4S. Similar effects were found with the slowly-inactivating CH4 chimera (see *right panel*). *C*, Confocal images of a middle plane of tsA 201 cells expressing the various chimera and immunostained with an anti-β antibody. After expression in cells, the CD8-β_2C3,4S chimera was also targeted to the membrane as the slowly inactivating wild-type β_{2a}, CH4, and CD8-CH4-C3,4S subunits. The CH4-C3,4S subunit was localized to the cytoplasm.

current inactivation and localizes the subunit to the cytoplasm, whereas addition of the CD8 segment restores both slow inactivation and membrane localization (Fig. 3*B*,*C*, *CH4-C3,4S*, *CD8-CH4-C3,4S*). The latter results suggest that the β_{2a} subunit needs a membrane anchor to reduce channel inactivation.

Another important feature of the α_{1A} channel properties recorded in the presence of the β_{2a} subunit is the shift in inactivation toward more depolarized values. Analysis of the inactivation properties of channels expressed with a β_{2a} subunit evidenced a depolarizing shift of ~10–20 mV in the half-inactivation potential ($E_{0.5}$) compared with channels containing a β_1 subunit. This difference was also found in our experimental conditions (BAPTA-injected oocytes) between oocytes expressing an α_{1A} plus α_2-δ plus β_{1b} or α_{1A} plus α_2-δ plus β_{2a} subunit combination ($E_{0.5}$ of -32 ± 5 and -13 ± 6 mV for β_{1b} and β_{2a}, respectively) (Fig. 4) . β subunit constructs that induced slowly inactivating currents also shifted the $E_{0.5}$ toward positive values (more than -20 mV) (Fig. 4, β_2, β*CH4*, *R10A*, *R13A*, *CD8-*β_2*C3,4S*, *CD8-CH4-C3,4S*). Conversely, β subunits producing fast inactivation (β_{1b}, β_2C3,4S, β_2C3S, and CH4-C3,4S) generated more hyperpolarized steady-state inactivation curves ($E_{0.5}$ of less than -20 mV). Interestingly, expression of the β_2R9–11A subunit, which induced currents characterized by a moderate percentage of inactivation, had an $E_{0.5}$ value intermediate between those observed for the β_{1b} and the β_{2a} subunits. The β_2C4S mutant was the only exception to this set of observations. The localization of this subunit was cytoplasmic and it induced rapidly inactivating currents (Fig. 3), but, contrary to expectations, the voltage dependence of inactivation was depolarized, similar to the β_{2a} subunit (-16 ± 1 mV). However, we conclude that, overall, a strong correlation appears to exist between the ability of these subunits to induce currents with slow kinetics and depolarized inactivation and their membrane localization.

We then analyzed the effects of the N terminal tail of β_{2a} directly on Ca^{2+} channel inactivation. This was done by injecting, 4 hr before recording, the V1β_2 peptide (corresponding to the first 16 amino acids of the β_{2a} subunit) (Fig. 5) into oocytes expressing the α_{1A}, α_2-δ, and β_1TF1 subunit combination. The final concentration of the peptide was estimated to be ~0.1 mM. Ba^{2+} currents recorded from both control noninjected and V1β_2-injected oocytes inactivated rapidly, as seen on the superimposed traces and histograms in Figure 5 (94 ± 2 and 88 ± 4% for injected and control oocytes, respectively). Injection of the peptide therefore did not modify the inactivation kinetics of the currents, although the combined presence of β_1TF1 and the V1β_2 peptide mimicked the βCH4 chimera, which produced slowly inactivating currents (Fig. 3). These results suggest that the presence of the N-terminal tail of β_2 in the cell is not sufficient, by itself, to induce slowing of inactivation. A physical link between the membrane-anchored N-terminal tail of β_2 (MAS) and the rest of the β subunit appears to be required to observe a slowing in inactivation. This link could be expected to restrict the mobility of the α_1 Ca channel I–II loop (AI–AII) (Fig. 6), which interacts directly with the β subunit. In these conditions, formation of the inactivated state of the channel may involve the binding of the I–II loop to a receptor site located on the intracellular side of the channel. We therefore searched for such potential interactions between the I–II loop and other intracellular domains of the channel. Different N- and C-terminal segments, as well as the II–III and the III–IV intracellular loops of the α_{1A} subunit, were constructed as GST fusion, produced, and purified (Fig. 6*B*, Coomassie blue-stained SDS-PAGE analysis of the GST fusion protein used). The different GST fusion proteins were then immobilized on glutathione agarose beads, incubated with *in vitro*-translated ^{35}S-labeled α_{1A} I–II loop, washed, and analyzed by SDS-PAGE and autoradiography. As seen in Figure

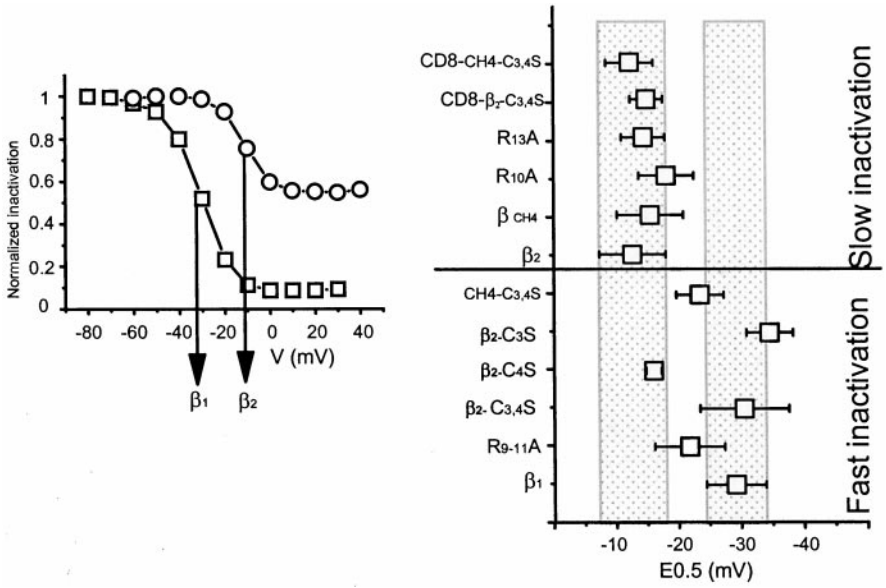

Figure 4. Membrane association of the β subunit shifts the steady-state inactivation relationship. *Left*, Typical steady-state inactivation curves recorded from oocytes expressing α_{1A} plus α_2-δ plus β_1 (labeled β_1) or α_{1A} plus α_2-δ plus β_2 (labeled β_2) subunits. Half-inactivation potentials were −32 and −12 mV for β_{1b} and β_{2a}, respectively. *Right*, Half-inactivation potentials obtained from oocytes expressing the α_{1A} plus α_2-δ subunits with different mutated or chimeric β subunits (n = 5–20). β subunits that induced slowly, β_{2a}-like, inactivating currents induced depolarized half-inactivation potentials. *Shadowed boxes* underline the values and SDs of the half-inactivation potentials for β_{1b} and β_{2a} subunits.

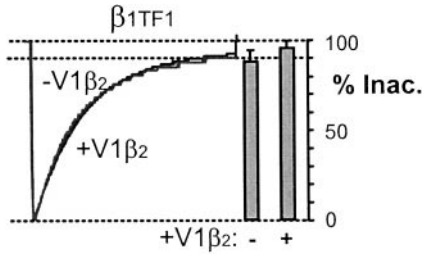

Figure 5. Perfusion of V1β_{2a} peptide does not accelerate inactivation. We injected the V1β_{2a} peptide (50 mM in H_20; final intra oocyte concentration of ~0.1 mM; see Fig. 2*A* for sequence) into oocytes expressing the α_{1A} and α_2-δ subunit with the β_{1b} subunit truncated in this V1 domain (β_1TF1). The combination (V1β_{2a} plus β_1TF1) corresponds to the two parts of chimera β-CH4, which induced slowly inactivating current when expressed with α_{1A} subunit. Currents were recorded during a typical test pulse to +10 mV in V1β_{2a}-injected (n = 6) and noninjected oocytes (n = 12). No statistical differences were seen in the inactivation kinetics between these two batches of oocytes, indicating that the V1β_{2a} peptide had no direct effect on channel inactivation.

6*C*, the α_{1A} I–II loop interacts with several intracellular domains, including the loop connecting domain III to IV (III–IV loop) and the N-terminal (NT6) and C-terminal (CT1, CT6) tails of the α_1 subunit. These sequences may thus be involved in the formation of the receptor site of the inactivation particle.

DISCUSSION

Ca^{2+} channel inactivation influences not only cellular excitability but also different Ca-dependent pathways leading to contraction, secretion, synaptic activation, or gene transcription. A large number of mutational studies have pointed out the important role played by multiple elements of the α_1 pore-forming subunit on channel inactivation (Zhang et al., 1994; de Leon et al., 1995; Klockner et al., 1995; Parent et al., 1995; Adams and Tanabe, 1997; Herlitze et al., 1997; Sokolov et al., 1999; Spaetgens and Zamponi, 1999). It has been shown, for example, that the IS6, I–II loop, and C-terminal part of the α_1 subunit are critical determinants for inactivation kinetics (Zhang et al., 1994; Herlitze et al., 1997; Bourinet et al., 1999; Cens et al., 1999a; Spaetgens and Zamponi, 1999). Overall, these studies strongly suggest that several interactions occur between multiple structural motifs of the channel during the transition between the open and the inactivated states of the channel. Additionally, the β subunits have also been shown to be directly involved in the modulation of channel inactivation and are therefore likely to represent key components of the molecular mechanism that leads to channel inactivation.

Our first finding that palmitoylation of Cys3 and Cys4 of the β_{2a} subunit is responsible for the β_{2a}-induced slowing of inactivation of the P/Q type Ca^{2+} channel extends previous reports of the effects of β_{2a} palmitoylation on α_{1E} and α_{1C} Ca^{2+} channels (Chien et al., 1996; Qin et al., 1998). The slowing of α_{1A} Ca^{2+} channel inactivation was correlated to a membrane localization of the β_{2a} subunit when expressed alone in tsA 201 cells. Both effects were suppressed by mutation of a single Cys residue (3 or 4), showing for the first time that the two Cys residues are necessary for slowing inactivation and producing membrane localization. Similarly, whereas mutation of single positively charged residues (Arg to Ala) at positions 9 and 13 was without effect on channel inactivation (Fig. 2), similar mutations of the three contiguous Arg at positions 9–11 strongly reduced channel inactivation and membrane localization. This effect may arise from structural modifications in the N-terminal tail of β_{2a} preventing subunit palmitoylation. Alternatively, electrostatic interactions between the acidic phospholipids and the cluster of basic residues could provide the energy necessary for membrane association of the subunit, as already shown for Src (Murray et al., 1998). In this case, hydrophobic and electrostatic interactions may act in synergy to target the β_{2a} subunit to the membrane. Further experimental analysis of the level of palmitoylation of the β_2R9–11A mutant will help to clarify the mechanism of targeting of the β_2 subunit. However, it should be noted that the inactivation kinetics recorded with the β_2R9–11A subunit, although being faster than those recorded with the wild-type β_{2a} subunit, were still slower than with the nonpalmitoylated, cytoplasmically localized β_2C3,4S subunit, suggesting that functional differences still exist between these two subunits. Our results define a minimal sequence (or MAS) for β_{2a} subunit targeting, in which Cys3, Cys4, and adjacent Arg (10 and 12) are key residues: M-CC——R-R–.

Another important clue to understand the role of the β_{2a} subunit in the modulation of inactivation is provided by the βCH4 chimera. In the βCH4 chimera, addition of the first 16 amino acids of β_{2a}, in place of the V1 domain of β_{1b} (Fig. 1*A*), induced palmitoylation (Chien et al., 1998), membrane localization of the chimera, and slowing of inactivation in coexpression experiments. This β_{2a}-V1 sequence can therefore act as a MAS independently of any other β_{2a}-specific sequences. However, effects of deletion of this MAS domain in the β_{2a} subunit, which prevents palmitoylation, induces relocalization of the subunit to the cytoplasm, and acceleration of inactivation, are not compensated by injection of the V1 domain of β_{2a} (Fig. 5). The latter results suggest that V1/MAS cannot act on its own to modulate channel inactivation but rather needs to be linked to a structural element common to β_1 (see results with βCH4) and β_{2a}. One obvious candidate is the β interaction domain

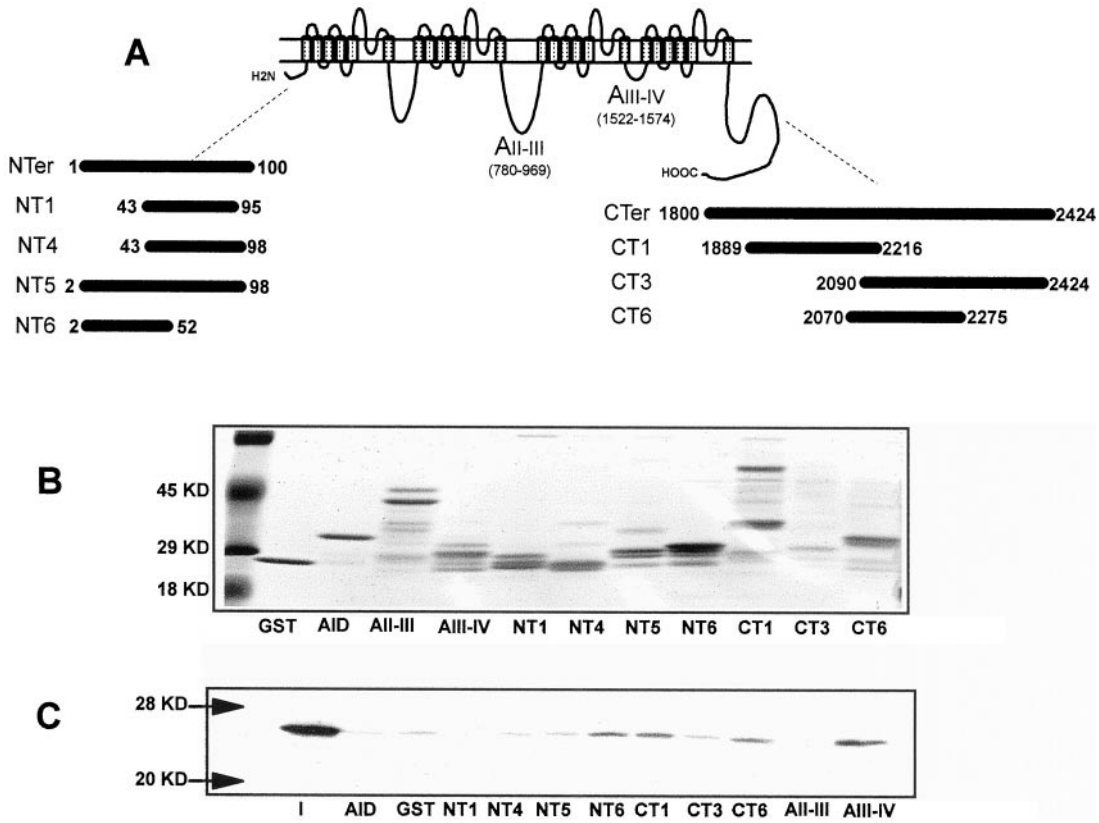

Figure 6. The α_{1A} Ca channel I–II loop interacts with multiple intracellular domains of the channel. Schematic localization (*A*) and Coomassie blue-stained SDS-PAGE (*B*) of the purified GST proteins fused to N-terminal (*NT1*, *NT4*, *NT5*, *NT6*), C-terminal (*CT1*, *CT3*, *CT6*) or intracellular loop (*AII-III*, *AIII-IV*, *AID*) sequences of the α_{1A} subunit. *C*, Specific association of ^{35}S-labeled I–II loop with N- and C-terminal sequences and III–IV loop of the channel. *I*, Input (2 μl of *in vitro* translated ^{35}S-labeled I–II loop); *GST*, control GST.

(BID) sequence (De Waard et al., 1994) located on C2, conserved in all β subunits, and directly responsible for the interaction between α_1 and β subunits. In our view, palmitoylation of Cys3,4 and binding to BID would act in concert to attenuate channel inactivation. The slowing in inactivation kinetics observed with the CD8-βC3,4S and CD8-CH4C3,4S chimera suggests in fact that the role of palmitic acid is solely to provide an MAS to the β subunit because addition of a transmembrane segment appears equally effective. The direct involvement of the I–II loop of the α_{1A} subunit in channel inactivation (Herlitze et al., 1997; Bourinet et al., 1999; Spaetgens and Zamponi, 1999) leads us to propose that this sequence may behave as an inactivation particle, directly responsible for channel occlusion after opening. We suggest that, owing to its two functional domains, the β_{2a} subunit acts as a molecular groom for the channel inactivation gate and immobilizes this inactivation particle by linking it to the membrane (Fig. 7). The model is compatible with the effect of the CD8-β_2C3,4S chimera, the effects of mutation on the I–II loop, and the acceleration of α_{1A} channel inactivation recorded during overexpression of this loop (Cens et al., 1999a). Such an immobilization of the inactivation particle in the open configuration should increase the free energy necessary to reach the inactivated state. It is thus expected to shift the steady-state inactivation curve toward depolarized potential values. This effect is indeed recorded with the β_{2a} subunit [half-inactivation potential ($E_{0.5}$), 15 mV more depolarized than with β_1] but also with its functional analog the CD8-β_2C3,4S or the βCH4 chimera. Conversely, release of the inactivation particle produces a shift of voltage-dependent inactivation toward more hyperpolarized potentials (see mutations β_2C3,4S and β_2C3S). The depolarized inactivation potential recorded with the rapidly inactivating β_2C4S subunit cannot be explained in this context. This particular mutation may prevent inactivation occurring from the closed state of the channel as opposed to other rapidly inactivating channels, without modifying the stability of the inactivated state. Similar modifications have already been reported for mutated Na^+ channels (Hartmann et al., 1994). The complete understanding of the effect of this mutation awaits recordings at the single-channel level and the knowledge of the palmitoylation state of all these mutant subunits.

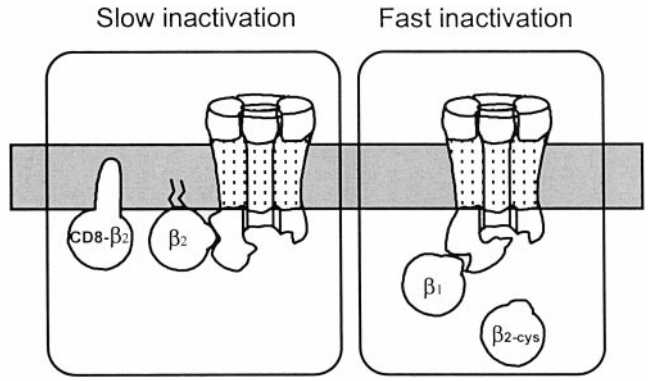

Figure 7. Proposed mechanism for β_{2a}-induced slowing of inactivation. In our scheme, the β_{2a} subunit works as a rigid link between the membrane (via a palmitic acid anchor) and the inactivating particle (via its BID domain). When this link is broken (e.g., in mutation β_2C3,4S, in a physiological situation producing a depalmitoylation, or in the case of a nonpalmitoylated β subunit), the inactivating particle (I–II loop) can move freely and produce the typical fast inactivation.

As expected, none of these mutations affected the interaction between the α_{1A} and the β subunit, because all are membrane localized when expressed with the α_{1A} subunit (data not shown). The GST pull-down experiment, shown in Figure 6, suggests multiple possible receptor sites for this inactivation particle. N-terminal and C-terminal sequences have already been shown to be involved in voltage- or calcium-dependent channel inactivation or regulation by β subunits. Interestingly, interaction of the I–II

loop appears to be stronger with the III–IV loop, the most conserved connecting loop among high voltage-activated Ca channels (α_{1A}, α_{1B}, α_{1C}, and α_{1E}; >70% of similarity). These channels all display a slowing of inactivation by the β_{2a} subunit. This loop is therefore a prime candidate for future studies on the inactivation mechanism, although other intracellular or intrapore domains may also directly participate in the process of inactivation.

The sensitivity of the thioester bond linking the palmitic acid to the β_{2a} subunits makes this site a potentially important pathway for the regulation of Ca^{2+} entry into cells. Reducing agents or membrane receptor activation are known to modify the palmitoylated state of some signaling proteins (G_α-protein and β-adrenergic receptor) (Casey, 1995; Peterson and Catterall, 1995). Recently, nitrosylation by nitric oxide of thiol groups on cysteine residues of the β-adrenergic receptor has been reported (Adam et al., 1999). Whether a similar pathway can affect palmitoylation of the β_{2a} subunit *in vivo* is not known but could potentially be important in physiological or pathological situations during ischemia or oxidative stress, for example. This phenomena would be restricted to β_{2a}-containing channels and would decrease calcium entry by promoting channel inactivation. In this respect, our results open new perspectives for further studies of the control of calcium channel inactivation by β_{2a} subunits, in particular in their native cellular environment.

REFERENCES

Adam L, Bouvier M, Jones TL (1999) Nitric oxide modulates beta(2)-adrenergic receptor palmitoylation and signaling. J Biol Chem 274:26337–26343.

Adams B, Tanabe T (1997) Structural regions of the cardiac Ca channel alpha subunit involved in Ca-dependent inactivation. J Gen Physiol 110:379–389.

Berrow NS, Brice NL, Tedder I, Page KM, Dolphin AC (1997) Properties of cloned rat alpha1A calcium channels transiently expressed in the COS-7 cell line. Eur J Neurosci 9:739–748.

Birnbaumer L, Qin N, Olcese R, Tareilus E, Platano D, Costantin J, Stefani E (1998) Structures and functions of calcium channel beta subunits. J Bioenerg Biomembr 30:357–375.

Bourinet E, Soong TW, Sutton K, Slaymaker S, Mathews E, Monteil A, Zamponi GW, Nargeot J, Snutch TP (1999) Splicing of alpha 1A subunit gene generates phenotypic variants of P- and Q-type calcium channels. Nat Neurosci 2:407–415.

Casey PJ (1995) Protein lipidation in cell signaling. Science 268:221–225.

Cens T, Mangoni ME, Richard S, Nargeot J, Charnet P (1996) Coexpression of the beta2 subunit does not induce voltage- dependent facilitation of the class C L-type Ca channel. Pflügers Arch 431:771–774.

Cens T, Restituito S, Vallentin A, Charnet P (1998) Promotion and inhibition of L-type Ca2+ channel facilitation by distinct domains of the subunit. J Biol Chem 273:18308–18315.

Cens T, Restituito S, Galas S, Charnet P (1999a) Voltage and calcium use the same molecular determinants to inactivate calcium channels. J Biol Chem 274:5483–5490.

Cens T, Restituito S, Charnet P (1999b) Regulation of Ca-sensitive inactivation of a 1-type Ca2+ channel by specific domains of beta subunits. FEBS Lett 450:17–22.

Chien AJ, Carr KM, Shirokov RE, Rios E, Hosey MM (1996) Identification of palmitoylation sites within the L-type calcium channel beta2a subunit and effects on channel function. J Biol Chem 271:26465–26468.

Chien AJ, Gao T, Perez Reyes E, Hosey MM (1998) Membrane targeting of L-type calcium channels. Role of palmitoylation in the subcellular localization of the beta2a subunit. J Biol Chem 273:23590–23597.

de Leon M, Wang Y, Jones L, Perez Reyes E, Wei X, Soong TW, Snutch TP, Yue DT (1995) Essential Ca(2+)-binding motif for Ca(2+)-sensitive inactivation of L-type Ca2+ channels. Science 270:1502–1506.

De Waard M, Pragnell M, Campbell KP (1994) Ca2+ channel regulation by a conserved beta subunit domain. Neuron 13:495–503.

De Waard M, Witcher DR, Pragnell M, Liu H, Campbell KP (1995) Properties of the alpha 1-beta anchoring site in voltage- dependent Ca2+ channels. J Biol Chem 270:12056–12064.

Hartmann HA, Tiedeman AA, Chen SF, Brown AM, Kirsch GE (1994) Effects of III-IV linker mutations on human heart Na+ channel inactivation gating. Circ Res 75:114–122.

Herlitze S, Hockerman GH, Scheuer T, Catterall WA (1997) Molecular determinants of inactivation and G protein modulation in the intracellular loop connecting domains I and II of the calcium channel alpha1A subunit. Proc Natl Acad Sci USA 94:1512–1516.

Jones LP, Wei SK, Yue DT (1998) Mechanism of auxiliary subunit modulation of neuronal alpha1E calcium channels. J Gen Physiol 112:125–143.

Klockner U, Mikala G, Varadi M, Varadi G, Schwartz A (1995) Involvement of the carboxyl-terminal region of the alpha 1 subunit in voltage-dependent inactivation of cardiac calcium channels. J Biol Chem 270:17306–17310.

Mangoni ME, Cens T, Dalle C, Nargeot J, Charnet P (1997) Characterisation of alpha1A Ba2+, Sr2+ and Ca2+ currents recorded with ancillary beta1–4 subunits. Receptors Channels 5:1–14.

Murray D, Hermida-Matsumoto L, Buser CA, Tsang J, Sigal CT, Ben Tal N, Honig B, Resh MD, McLaughlin S (1998) Electrostatics and the membrane association of Src: theory and experiment. Biochemistry 37:2145–2159.

Neely A, Wei X, Olcese R, Birnbaumer L, Stefani E (1993) Potentiation by the beta subunit of the ratio of the ionic current to the charge movement in the cardiac calcium channel. Science 262:575–578.

Olcese R, Qin N, Schneider T, Neely A, Wei X, Stefani E, Birnbaumer L (1994) The amino terminus of a calcium channel beta subunit sets rates of channel inactivation independently of the subunit's effect on activation. Neuron 13:1433–1438.

Parent L, Gopalakrishnan M, Lacerda AE, Wei X, Perez Reyes E (1995) Voltage-dependent inactivation in a cardiac-skeletal chimeric calcium channel. FEBS Lett 360:144–150.

Perez Reyes E, Schneider T (1994) Calcium channels: structure, function and classification. Drug Dev Res 33:295–318.

Perez Reyes E, Castellano A, Kim HS, Bertrand P, Baggstrom E, Lacerda AE, Wei XY, Birnbaumer L (1992) Cloning and expression of a cardiac/brain beta subunit of the L-type calcium channel. J Biol Chem 267:1792–1797.

Peterson BZ, Catterall WA (1995) Calcium binding in the pore of L-type calcium channels modulates high affinity dihydropyridine binding. J Biol Chem 270:18201–18204.

Pichler M, Cassidy TN, Reimer D, Haase H, Kraus R, Ostler D, Striessnig J (1997) Beta subunit heterogeneity in neuronal L-type Ca2+ channels. J Biol Chem 272:13877–13882.

Pragnell M, Sakamoto J, Jay SD, Campbell KP (1991) Cloning and tissue-specific expression of the brain calcium channel beta-subunit. FEBS Lett 291:253–258.

Pragnell M, De Waard M, Mori Y, Tanabe T, Snutch TP, Campbell KP (1994) Calcium channel beta-subunit binds to a conserved motif in the I-II cytoplasmic linker of the alpha 1-subunit. Nature 368:67–70.

Qin N, Platano D, Olcese R, Costantin JL, Stefani E, Birnbaumer L (1998) Unique regulatory properties of the type 2a Ca2+ channel beta subunit caused by palmitoylation. Proc Natl Acad Sci USA 95:4690–4695.

Randall A, Benam CD (1999) Recent advances in the molecular understanding of voltage-gated Ca^{2+} channels. Mol Cell Neurosci 14:255–272.

Sather WA, Tanabe T, Zhang JF, Mori Y, Adams ME, Tsien RW (1993) Distinctive biophysical and pharmacological properties of class A (BI) calcium channel alpha 1 subunits. Neuron 11:291–303.

Sokolov S, Weiss RG, Kurka B, Gapp F, Hering S (1999) Inactivation determinant in the I-II loop of the Ca2+ channel alpha1-subunit and beta-subunit interaction affect sensitivity for the phenylalkylamine (−)gallopamil. J Physiol (Lond) 519:315–322.

Spaetgens RL, Zamponi GW (1999) Multiple structural domains contribute to voltage-dependent inactivation of rat brain alpha(1E) calcium channels. J Biol Chem 274:22428–22436.

Starr TV, Prystay W, Snutch TP (1991) Primary structure of a calcium channel that is highly expressed in the rat cerebellum. Proc Natl Acad Sci USA 88:5621–5625.

Stea A, Dubel SJ, Pragnell M, Leonard JP, Campbell KP, Snutch TP (1993) A beta-subunit normalizes the electrophysiological properties of a cloned N-type Ca2+ channel alpha 1-subunit. Neuropharmacology 32:1103–1116.

Stea A, Tomlinson WJ, Soong TW, Bourinet E, Dubel SJ, Vincent SR, Snutch TP (1994) Localization and functional properties of a rat brain alpha 1A calcium channel reflect similarities to neuronal Q- and P-type channels. Proc Natl Acad Sci USA 91:10576–10580.

Varadi G, Lory P, Schultz D, Varadi M, Schwartz A (1991) Acceleration of activation and inactivation by the beta subunit of the skeletal muscle calcium channel. Nature 352:159–162.

Walker D, De Waard M (1998) Subunit interaction sites in voltage-dependent Ca2+ channels: role in channel function. Trends Neurosci 21:148–154.

Zhang JF, Ellinor PT, Aldrich RW, Tsien RW (1994) Molecular determinants of voltage-dependent inactivation in calcium channels. Nature 372:97–100.